Journal of the European Ceramic Society 21 (2001) 2199–2205

www.elsevier.com/locate/jeurceramsoc

Ferroelectric SBN thin films grown by an SBN/Bi_2O_3 PLD sequential process

S.M. Zanetti [a], J.R. Duclere [b], M. Guilloux-Viry [b], V. Bouquet [a], E.R. Leite [a], E. Longo [a,*], J.A. Varela [c], A. Perrin [b]

[a] *Departamento de Química, Universidade Federal de São Carlos, UFSCar, PO Box 676, 13560-905 São Carlos, SP, Brazil*
[b] *Laboratoire de Chimie du Solide et Inorganique Moléculaire, UMR 6511 CNRS/Université de Rennes 1, Institut de Chimie de Rennes, Campus de Beaulieu, 35042 Rennes Cedex, France*
[c] *Instituto de Química, Universidade Estadual de São Paulo, UNESP, PO Box 355, 14801-970 Araraquara, SP, Brazil*

Received 13 September 2000; accepted 16 October 2000

Abstract

Ferroelectric $SrBi_2Nb_2O_9$ (SBN) thin films were prepared by pulsed laser deposition (PLD) on Pt/Ti/SiO_2/Si(100) using a sequential deposition process from two SBN and Bi_2O_3 targets. This route allows for bismuth enrichment of the film composition in order to improve the ferroelectric characteristics. Structural and microstructural characterizations were performed by X-ray diffraction (XRD) and scanning electron microscopy (SEM). The composition of films and targets was determined by energy dispersive X-ray spectrometry (EDX). The deposition temperature, which provided well-crystallized layered perovskite SBN phase films in situ, was found to be 700°C. The results were compared with those obtained for SBN films deposited at 400°C and then crystallized ex situ. For an ex situ annealing temperature of 750°C, a remanent polarization value (Pr) of 23.2 μc/cm^2 and a coercive field (Ec) of 112 kV/cm were measured.

Keywords: Ferroelectric properties; Films; PLD; Pulsed laser deposition; $SrBi_2Nb_2O_9$

1. Introduction

Ferroelectric thin films have received a great deal of attention in recent years due to their potential application in microelectronics, particularly as materials for nonvolatile memories (FERAM).[1] The most exhaustively studied compound for this application has been $Pb(Zr,Ti)O_3$ (PZT); however, a serious problem involving degradation after a number of cycles of polarization, known as "fatigue", has limited the application of PZT.[2] Candidate materials to control the problem of fatigue are those belonging to the bismuth-layered perovskite family, $(A_{m-1}B_mO_{3m+1})^{2+}(Bi_2O_2)^{2-}$, such as $SrBi_4Ti_4O_{15}$ (SBIT), $SrBi_2Ta_2O_9$ (SBT) and $SrBi_2Nb_2O_9$ (SBN). Among the several bismuth-layer compounds, SBT and SBN have been intensively studied due to their high dielectric constant, low leakage current and good ferroelectric characteristics. Several methods have been employed in the preparation of SBT and SBN thin films, such as sol-gel,[3,4] MOD,[5,6] rf sputtering,[7] pulsed laser deposition,[8] polymeric precursors,[9] etc.

Control of the composition in terms of the volatility of bismuth and the presence of second phases constitute the main limitations of the Sr–Bi–Nb–O[10] system. Among the solutions proposed to compensate for the Bi loss which can occur during deposition or annealing are, generally, the use of Bi-enriched targets and, in some cases, Bi_2O_3-inserted heterostructures[11,12] for SBT or SBTN films.

In this paper, we report on SBN thin films deposited by PLD. A sequential deposition from two SBN and Bi_2O_3 targets was attempted to control the composition and to improve the ferroelectric characteristics.

2. Experimental

2.1. Preparation by pulsed laser deposition

The films were grown in situ by pulsed laser deposition (PLD) from SBN and Bi_2O_3 targets of approximately

* Corresponding author.
E-mail address: psmz@iris.ufscar.br (E. Longo).

0955-2219/01/$ - see front matter
PII: S0955-2219(00)00304-6

20 mm diameter and 5 mm thickness. The SBN targets were prepared by solid state reaction using $SrCO_3$, Nb_2O_5 and Bi_2O_3 as starting reagents, which were mixed in a ball mill for 8 h in isopropanol. After drying, the mixed powder was subjected to calcination at 1100°C for 8 h, followed by 1 h in an attrition mill. Pellets were then prepared by uniaxial compression, followed by isostatic pressing and sintering at 1150°C for 2 h. The targets thus obtained exhibited densities of approximately 80% of the theoretical one.

An XeCl ($\lambda = 308$ nm) excimer laser source (SOPRA SEL 520) was used to ablate the rotating targets. The laser beam (pulses of 40 ns duration and repetition rate fixed at 2 Hz) was focused on the target surface (fluence of 3–4 J/cm^2) at an angle of 45°. The target-substrate distance was fixed at 40 mm. The films were deposited onto Pt/Ti/SiO_2/Si(100) substrates for a deposition time fixed at 20 min. The as-deposited films were typically 300–350 nm thick.

The influence of the deposition temperature was investigated in this study (the substrate holder temperature ranged from 550 to 750°C) as well as the influence of the oxygen pressure. Before deposition, the substrates were cleaned in acetone and mounted with silver paint on the stainless steel substrate holder.

2.2. Characterization

Structural characterizations were performed by XRD using an INEL CPS 120 diffractometer with a curved position-sensitive detector (Cu$K_{\alpha 1}$ radiation). The microstructure was examined with a field emission scanning electron microscope (FE–SEM) JEOL 6301 F operated at 7kV. Film and target composition was determined by EDX analysis with an ISIS Oxford device fitted onto a JEOL 6400 SEM. The thin films were analyzed at a low voltage (5 kV) to discard any possibility of substrate contribution.

The ferroelectric properties were measured using a Radiant tester RT6000HVS under virtual ground conditions. For this, an array of Au contacts, each with a nominal area of 7.1×10^{-4} cm^2, were sputter deposited using an appropriate shadow mask. Capacitance–voltage (C–V) characteristics were studied using an HP 4194A impedance analyser at a 100 kHz frequency.

3. Results and discussion

3.1. In situ deposited films from stoichiometric SBN targets

The thin films were deposited at various temperatures from a stoichiometric target. As illustrated by the XRD pattern in Fig. 1, the ceramic SBN target is single phase. The EDX analysis revealed that the virgin region of the target is stoichiometric, whereas the ablated region is bismuth-deficient (Table 1). The loss of bismuth can be attributed to the high temperature reached on the surface of the target during plasma formation, which leads to bismuth evaporation.

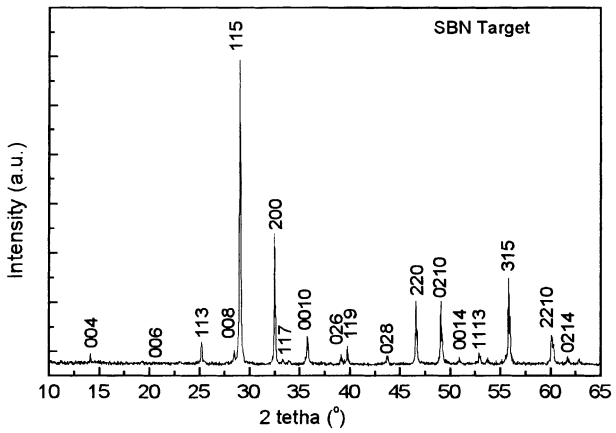

Fig. 1. XRD pattern for the SBN ceramic target sintered at 1150°C for 2 h.

Fig. 2 displays the diffraction patterns obtained for the films deposited from 550 to 750°C under 0.3 mbar oxygen pressure. The films deposited at 550 and 600°C show the presence of the so-called intermediate fluorite phase. This fluorite phase was observed by Rodriguez et al.[13] in SBT films and was also observed in SBN films prepared by the chemical method.[9] It should be pointed out that it is very difficult to distinguish between the intermediate fluorite phase and the layered perovskite phase because the positions of the peaks of both phases are very close. The peaks of the perovskite phase can be observed at 650°C, coexisting with the intermediate phase. As the deposition temperature increases, the intermediate phase disappears, whereas the perovskite phase is well crystallized at 700°C. The pyrochlore phase can also be detected as secondary phase. The degradation of the perovskite phase occurs at 750°C, probably due to the severe loss of bismuth (Sr/Bi/Nb was typically 1/0.6/2.5).

The FE–SEM micrographs (Fig. 3) reveal the strong influence of the deposition temperature on the film

Table 1
EDX results for SBN targets and films prepared by PLD at 700°C under various oxygen pressures

Sample		Sr (at.%)	Bi (at.%)	Nb (at.%)	Sr/Bi/Nb
Ceramic target					
Virgin region		20	41	39	1/2.0/1.9
Ablated region		28	20	52	1/0.7/1.8
SBN films: pO_2 =	0.05	29.5	8.5	62	1/0.3/2.11
	0.15	23.2	29.6	47.2	1/1.27/2.03
	0.30	20.5	35.7	43.8	1/1.75/2.14

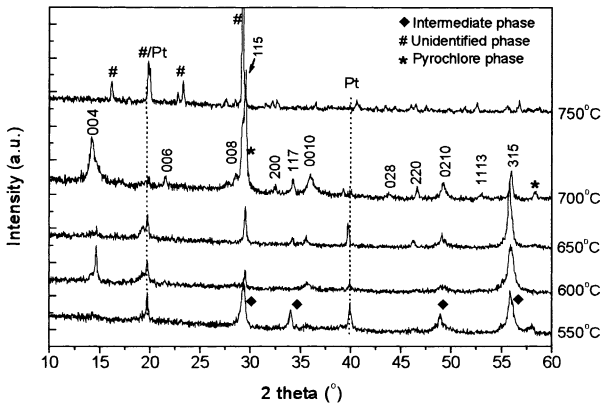

Fig. 2. XRD patterns for SBN films deposited by PLD under 0.3 mbar oxygen pressure at several temperatures.

microstructure. Although all the deposited films have a dense structure, the film deposited at 550°C shows a different grain microstructure with smaller spherical grains. These spherical grains are ascribed to the intermediate fluorite phase detected in the XRD pattern. As the temperature increases to 650°C, an increase in the grain size as well as a change in the grain shape, from spherical to angular form, can be observed. The small spherical grains are still present, probably due to the coexistence of the intermediate fluorite and the perovskite phases. A dense structure with angular grains (SBN phase) can be observed at 700°C.

The electrical characterizations were obtained through the capacitance versus voltage (C–V) curve recorded at 100 kHz frequency. Fig. 4 shows a comparison of the (C–V) curves between SBN films deposited at 700°C under 0.13 and 0.3 mbar oxygen pressures.

The film deposited at 0.13 mbar oxygen pressure (Fig. 4a) shows a paraelectric behavior that is ascribable to the high bismuth deficiency (Sr/Bi/Nb is 1/1.12/2.17). In contrast, the film deposited at 0.3 mbar oxygen pressure (Fig. 4b) shows a typical butterfly-like curve, characterizing a ferroelectric material. The asymmetry may be due to the off-stoichiometry of the film (Sr/Bi/Nb is 1/1.85/2.08). Although the bismuth deficiency is not as high as in the previous film (Fig. 4a), it suffices to create many defects that affect the electrical properties. The difference between the two maxima values of the capacitance at the positive and negative sides of bias is due to different electrode/film interfaces.

Despite the SBN crystallization obtained in situ at 700°C and 0.3 mbar oxygen pressure, the films are bismuth deficient, as is clearly illustrated in Table 1. This deficiency is responsible for the coexistence of a pyrochlore phase with SBN.

In order to prevent this loss of bismuth and to increase the ferroelectric performance,[14] a sequential deposition from SBN and Bi_2O_3 targets was tested. Both the in-situ and the ex-situ routes were compared.

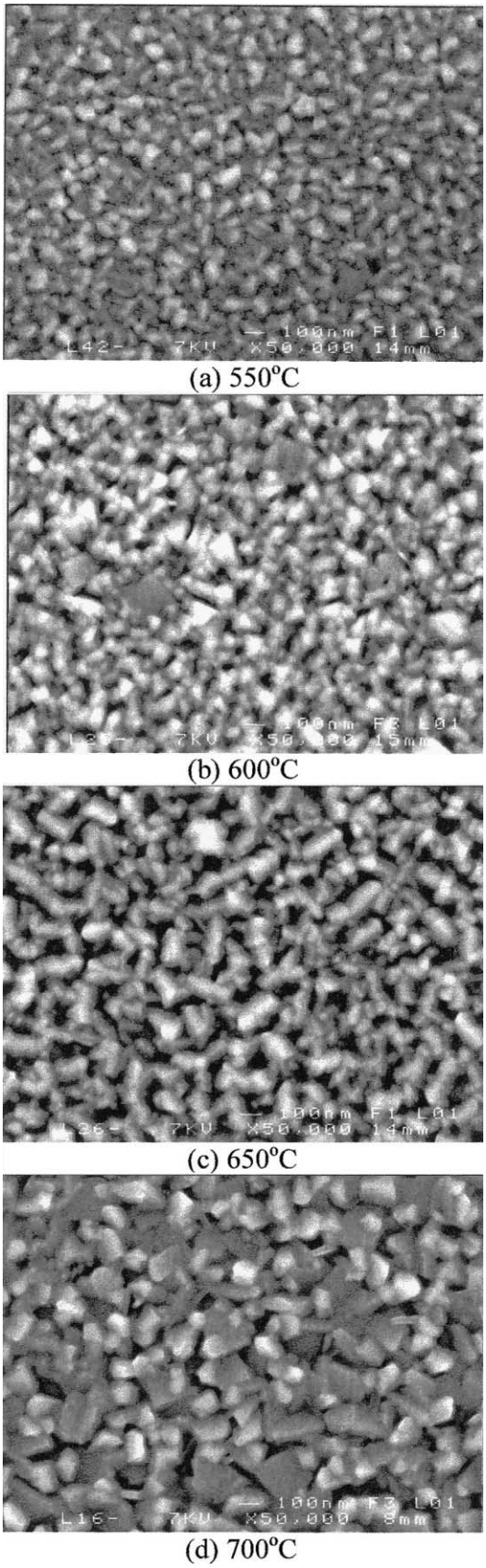

Fig. 3. FE–SEM micrographs for SBN thin films deposited on Pt/Si substrate by PLD at different temperatures.

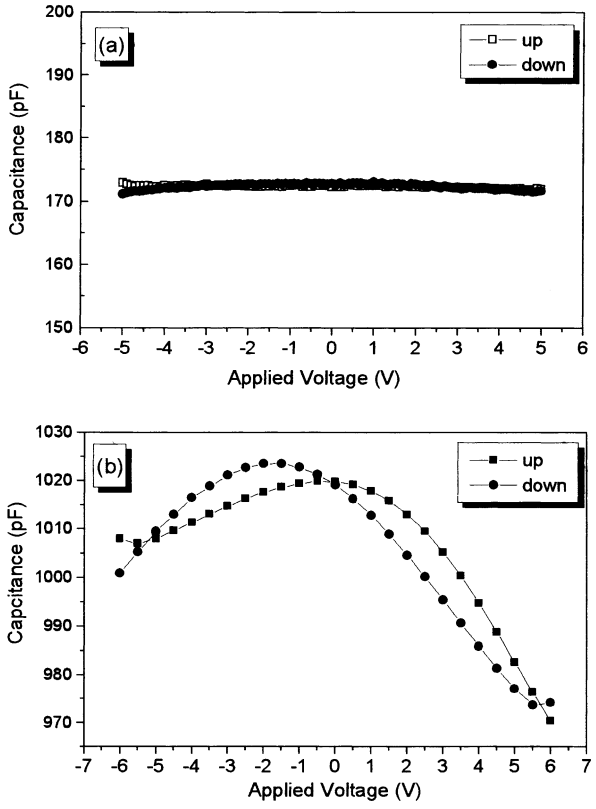

Fig. 4. C–V curves of SBN thin films deposited by PLD at 700°C under oxygen pressure of (a) 0.13 and (b) 0.3 mbar.

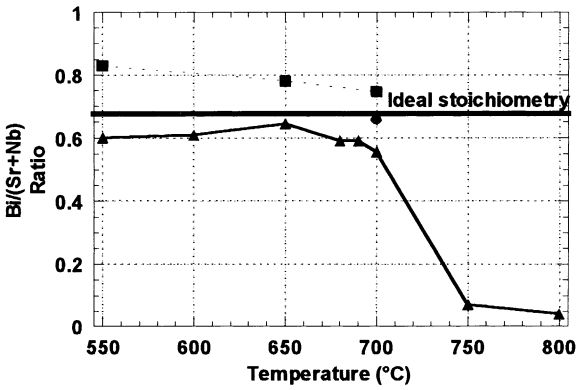

Fig. 5. Bi content (EDX data) of the films prepared from stoichiometric target (▲) and sequences of SBN/Bi_2O_3: (1000/100)×2 (●) and (500/100)×4 (■) pulses.

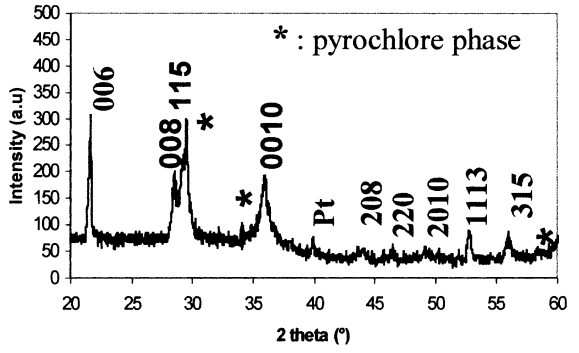

Fig. 6. XRD pattern of SBN thin film deposited with a sequence of SBN/Bi_2O_3 (1000/100)×2 at 700°C under 0.3 mbar oxygen pressure.

3.2. Thin films grown by the sequential deposition process

3.2.1. In situ route

The thin films were deposited at several temperatures under 0.3 mbar oxygen pressure using various SBN/Bi_2O_3 sequences. Fig. 5 illustrates the influence of the sequential deposition on the composition of the films.

Thin films with a close to stoichiometric composition can be synthesized in situ at 700°C, with deposition consisting of two sequences of 1000 SBN laser pulses followed by 100 pulses of Bi_2O_3. Fig. 6 displays the XRD pattern of a film obtained under these conditions, for which the Bi/(Sr + Nb) ratio is almost 0.66. A 00l preferential orientation is observed. This orientation, as reported by Lettieri et al.,[15] is detrimental to the ferroelectric performance because the remanent polarization lies in the (a,b) plane.

A small amount of a pyrochlore phase is still observed. This preferential orientation evidenced by XRD is in agreement with AFM and SEM observations (Fig. 7). Fig. 7 reveals growth of platelets characteristic of the 00l preferential orientation.

A film with a higher Bi content obtained with a different sequential deposition consisting of four sequences of 500 laser pulses of SBN, followed by 100 pulses of Bi_2O_3, was also characterized. Fig. 8 displays a (C–V) curve of this film. A much more symmetric butterfly-like curve can be observed than the one given in Fig. 4b. This behavior is due to the higher Bi content, in agreement with Chen et al.[14] Although the film presented a ferroelectric characterized (C–V) curve, the hysteresis loop could not be obtained due to a high dissipation factor (tan δ) at low frequencies, which interferes in measurements using the ferroelectric tester.

3.2.2. Ex situ route

To overcome the difficulties involved in in situ growth at 700°C, such as loss of bismuth and preferential orientation, an ex situ route was tested. The films were deposited from the stoichiometric target at 400°C and post annealed at the same temperature as that used for the in situ route (650, 700 and 750°C) in an oxygen atmosphere. This deposition temperature was chosen because the films do not adhere to the substrate at room temperature and, at a temperature above 400°C, the fluorite phase begins to nucleate. These films presented better electrical properties than those crystallized in situ, though not as good as those required for the applications. The SBN deposition alone, at 400°C without sequential deposition and followed by post-annealing is, in any case, insufficient to reach the ideal composition. In a case such as that, the films are still Bi-deficient. Therefore, an experiment was

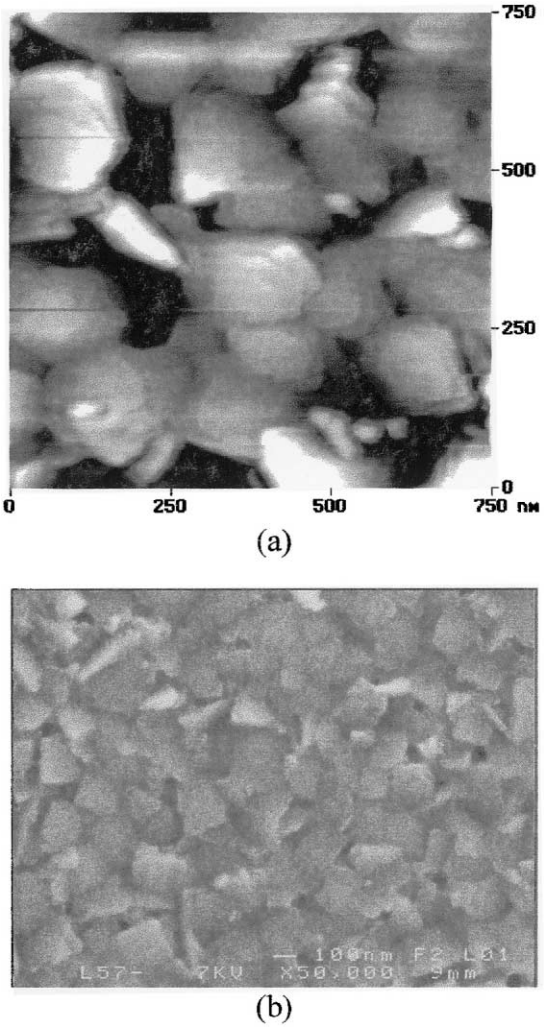

Fig. 7. AFM (a) and (b) SEM observations of SBN thin film deposited with a sequence of SBN/Bi_2O_3 (1000/100)×2 at 700°C under 0.3 mbar oxygen pressure.

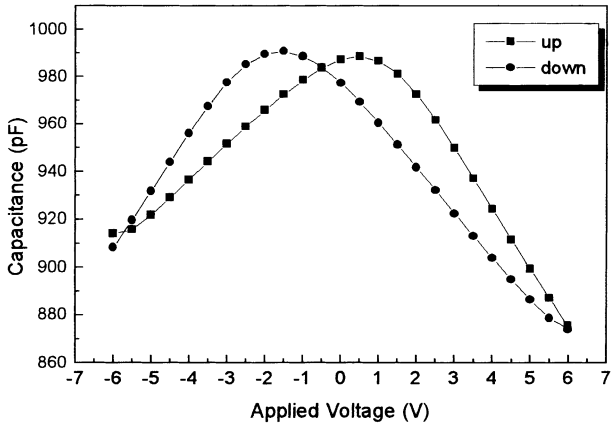

Fig. 8. (C–V) curve of a stoichiometric thin SBN film deposited by PLD with a sequence of SBN/Bi_2O_3 (500/100)×4 at 700°C under 0.3 mbar oxygen pressure.

carried out by the ex situ route, allied to sequential deposition from the stoichiometric SBN and Bi_2O_3 targets at 400°C under 0.3 mbar of oxygen in four sequences of 500 laser pulses of SBN, followed by 100 pulses of Bi_2O_3. These films were post-annealed, respectively, at 650, 700 and 750°C for 2 h in an oxygen atmosphere. Film thicknesses were typically around 300 nm.

Fig. 9 shows the hysteresis loops obtained at 60 Hz frequency at applied voltages of 5 and 10 V. The remanent polarization (Pr) and the coercive field (Ec) were 10.6 μC/cm^2 and 95 kV/cm, 14.7 μC/cm^2 and 158 kV/cm, and 23.2 μC/cm^2 and 112 kV/cm for the films crystallized at 650,

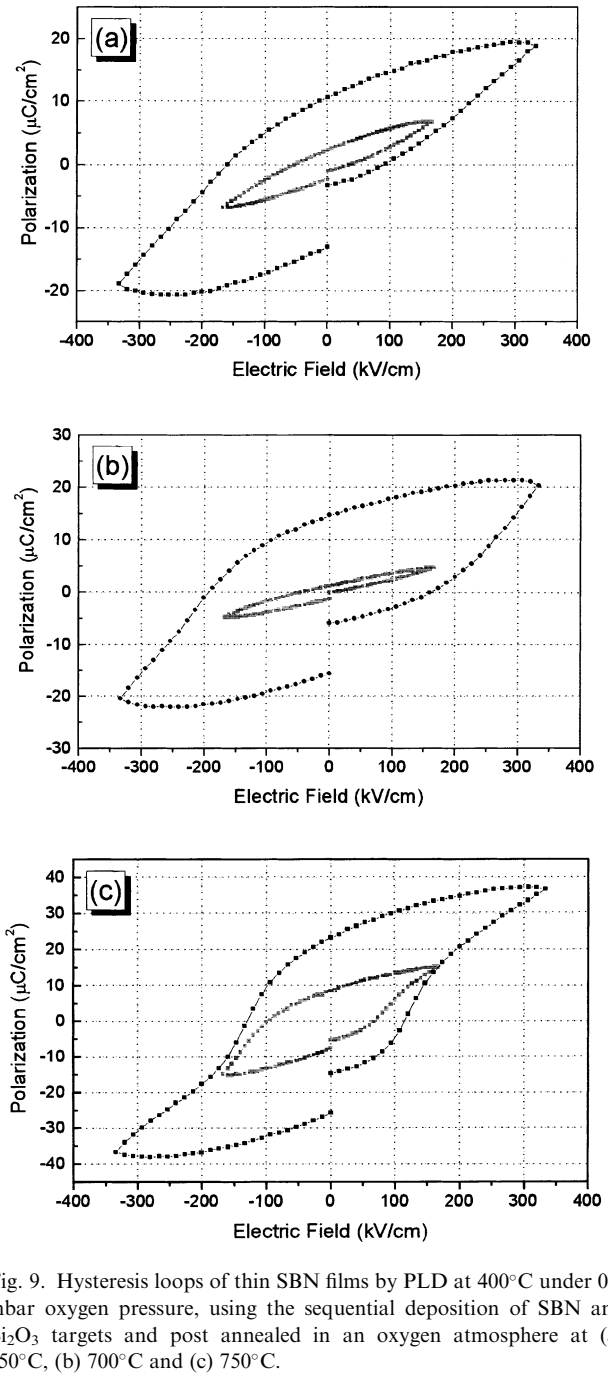

Fig. 9. Hysteresis loops of thin SBN films by PLD at 400°C under 0.3 mbar oxygen pressure, using the sequential deposition of SBN and Bi_2O_3 targets and post annealed in an oxygen atmosphere at (a) 650°C, (b) 700°C and (c) 750°C.

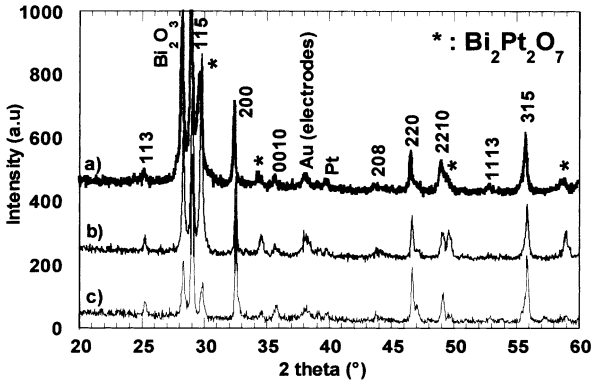

Fig. 10. XRD patterns for SBN films deposited by PLD at 400°C using the sequence of SBN/Bi_2O_3 (500/100)×4 pulses and post-annealed at: (a) 650°C, (b) 700°C, (c) 750°C, in an oxygen atmosphere.

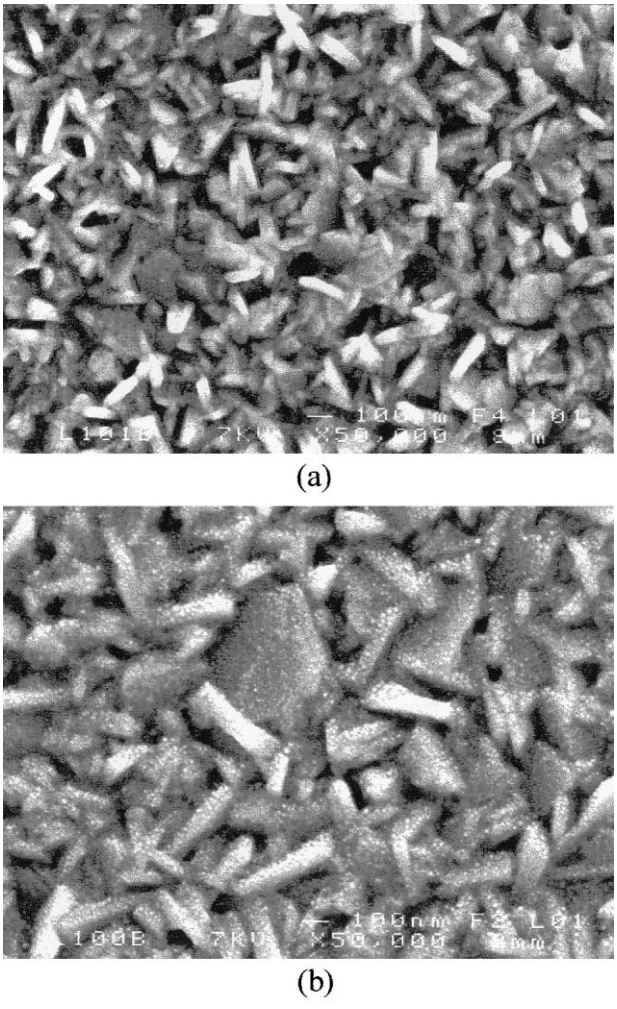

(a)

(b)

Fig. 11. Microstructure of SBN thin films prepared using the sequence of SBN/Bi_2O_3 (500/100)×4 pulses at 400°C under 0.3 mbar oxygen pressure and treated ex-situ at: (a) 700°C and (b) 750°C, in an oxygen atmosphere.

700 and 750°C, respectively, for an applied voltage of 10 V. These results are in good agreement with the published data[17] and evidence the efficiency of the ex situ sequential deposition process.

The evolution of the diffraction patterns was also studied and is presented in Fig. 10. For each temperature, it can be clearly seen that some Bi_2O_3 which did not react with SBN still remains. The segregation is related to the high excess of bismuth. At 750°C, the Bi_2O_3 contribution decreases, indicating better diffusion of the bismuth oxide in the SBN structure. This fact offers a partial explanation of the higher ferroelectric performances for this annealing temperature. Moreover, another pyrochlore phase ($Bi_2Pt_2O_7$), and possibly some $PtBi_2$ phase,[10] can be identified on each diffraction pattern, due to the reaction between the substrate and the high excess of bismuth. This pyrochlore phase is no longer associated to the bismuth deficiency.

Finally, no further (00l) preferential orientation is observed, which is in good agreement with the superior ferroelectric performance obtained with post annealing treatment. However, the crystallographic orientation is not the only reason for improved ferroelectric performance since a grain size effect is also involved.[16]

An observation of the microstructure in Fig. 11 reveals a strong difference in the mean grain size between SBN films deposited at 400°C and annealed at 700°C (Fig. 11a) and 750°C (Fig. 11b), which also partially explains the improvement of the ferroelectric performance. A comparison of the ex situ and in situ routes now indicates that the mean grain size of the films prepared ex situ (Fig. 11b) is almost 1.5 larger than that of the films prepared in situ (Fig. 7b).

4. Conclusions

The preparation of SBN thin films by the pulsed laser deposition method is presented herein. In agreement with the structural characterizations, the deposition temperature of 700°C gave rise to the ferroelectric SBN phase, as confirmed by observation of the (C–V) curves, although the film is Bi-deficient. An alternative route, consisting of the sequential deposition of SBN and Bi_2O_3 layers, was experimented to avoid the loss of bismuth in films prepared in situ.

The same procedure, using this alternative route, combined with deposition at a low temperature (400°C) and followed by post annealing ex situ, produced films with remanent polarization above 10 μc/cm^2. The Bi_2O_3 phase was still present after thermal treatment. Different sequences with shorter Bi_2O_3 deposition time may be experimented in order to decrease the excess of bismuth.

Acknowledgements

This work was financially supported by the Brazilian research agencies FAPESP, MCT/CNPq/PRONEX and CAPES/COFECUB. EDX data and FE–SEM micro-

graphs were collected at the Center for Scanning Electron Microscopy and Microanalysis (CMEBA) in the University of Rennes I.

References

1. Watanabe, H., Mihara, T., Yoshimori, H. and Paz de Araujo, C. A., *Jpn. J. Appl. Phys*., 1995, **34**, 5240.
2. Mihara, T., Yoshimori, H., Watanabe, H. and Paz de Araujo, C. A., *Jpn. J. Appl. Phys*., 1995, **34**, 5233.
3. Bae, K., Lee, H. S. and Cho, S. K., *J. Korean Physical Society*, 1998, **32**, S1565.
4. Ching-Prado, E., Perez, W., Reynés-Figueroa, A., Katiyar, R. S., Ravichandran, D. and Bhalla, A. S., *Mater. Res. Soc. Symp*., 1997, **459**, 213.
5. Joshi, P. C., Ryu, S. O., Zhang, X. and Desu, S. B., *J. Korean Physical Society*, 1998, **32**, S1583.
6. Mihara, T., Yoshimori, H., Watanabe, H. and Paz de Araujo, C. A., *Jpn. J. Appl. Phys*., 1995, **34**, 5233.
7. Lee, J.-K., Kim, T. S., Jung, H.-J., Cho, K.-J., Park, J.-W. and Kim, H. J., *J. Korean Physical Society*, 1998, **32**, S1550.
8. Oishi, Y., Matsumuro, Y. and Okuyama, M., *Jpn. J. Appl. Phys*., 1997, **36**, 5896.
9. Zanetti, S. M., Leite, E. R., Longo, E. and Varela, J. A., *J. Mater. Res*., 1998, **13**, 2392.
10. Park, Y.-B., Lee, J.-K., Jung, H.-J. and Park, J.-W., *J. Mater. Res*., 1999, **14**, 2986.
11. Park, Y.-B., Jang, S.-M., Lee, J.-K. and Park, J.-W., *J. Vac. Sci. Technol*., 2000, **A18**, 17.
12. Dinu, R., Dinescu, M., Pedarnig, J. D., Gunasekaran, R. A., Bauerle, D., Bauer-Gogonea, S. and Bauer, S., *Appl. Phys. A*, 1999, **69**, 55.
13. Rodriguez, M. A., Boyle, T. J., Hernandez, B. A., Buchheit, C. D. and Eatough, M. O., *J. Mater. Res*., 1996, **11**, 2282.
14. Chen, T.-C., Li, T., Zhang, X. and Desu, S. B., *J. Mater. Res*., 1997, **12**, 1569.
15. Lettieri, J., Jia, Y., Urbanik, M., Weber, C. J., Maria, J.-P., Schlom, D. G., Li, H., Ramesh, R., Uecker, R. and Reiche, P., *Appl. Phys. Lett*., 1998, **73**, 2923.
16. Nagata, M., Vijay, D. P., Zhang, X. and Desu, S. B., *Phys. Stat. Sol. (a)*, 1998, **157**, 75.
17. Battacharyya, S., Bharadwaja, S. S. N. and Krupanidhi, S. B., *Appl. Phys. Lett*., 1999, **75**, 2656.